Electromagnetic field structure and normal mode coupling in photonic crystal nanocavities

C. Dineen, J. Förstner, A.R. Zakharian, J.V. Moloney

ACMS at the Department of Mathematics, University of Arizona, Tucson AZ 85721, USA

cdineen@acms.arizona.edu

S.W. Koch

Department of Physics and Materials Sciences Center, Philipps University, Renthof 5, 35032 Marburg, Germany

Abstract: The electromagnetic field of a high-quality photonic crystal nanocavity is computed using the finite difference time domain method. It is shown that a separatrix occurs in the local energy flux discriminating between predominantly near and far field components. Placing a two-level atom into the cavity leads to characteristic field modifications and normal-mode splitting in the transmission spectra.

References and links

1. J.D. Joannopoulos, R.D. Meade, and J.N. Winn, *Photonic Crystals: Molding the Flow of Light* (Princeton Univ. Press, 1995)
2. T. Yoshie, A. Scherer, J. Hendrickson, G. Khitrova, H.M. Gibbs, G. Rupper, C. Ell, O.B. Shchekin, and D.G. Deppe, "Vacuum Rabi splitting with a single quantum dot in a photonic crystal nanocavity," Nature **432**, 200-203 (2004)
3. T. Yoshie, J. Vuckovic, A. Scherer, H. Chen, and D. Deppe, "High quality two-dimensional photonic crystal slab cavities," Appl. Phys. Lett. **79**, 4289 - 4291 (2001).
4. J. Vuckovic, M. Loncar, H. Mabuchi, and A. Scherer, "Design of photonic crystal microcavities for cavity QED," Phys. Rev. E **65**, 016608-1-11 (2001).
5. H. Haug and S.W. Koch, *Quantum Theory of the Optical and Electronic Properties of Semiconductors* 4th ed., (World Scientific, Singapore, 2004).
6. L. Allen and J.H. Eberly, *Optical Resonance and Two-Level Atoms*. (Dover, 1975)
7. A. Taflove and S.C. Hagness, *Computational Electrodynamics: the FDTD method* 2nd ed. (Artech House, Boston, London, 2000)
8. N. Kaneda, B. Houshmand, and T. Itoh, "FDTD Analysis of Dielectric Resonators with Curved Surfaces," IEEE Trans. on Microwave Theory and Techniques **45**, 1645-1649 (1997).
9. L. Mandel, and E. Wolf, *Optical coherence and quantum optics* (Cambridge Univ. Press, 1995)
10. P.R. Berman (Editor), *Cavity Quantum Electrodynamics* (Academic Press, San Diego, 1994)
11. Full versions of animations are available at: http://acms.arizona.edu/oe/

---

1. Introduction

High quality photonic crystal structures can be realized by a periodic arrangement of air holes in a dielectric medium [1]. Introducing appropriate defects into the structure makes it possible to design optical microcavities with mode volume diameters in the wavelength range and

very high quality (Q) factors. These microcavities are well suited to study non-perturbative light-matter coupling effects if one inserts an optically resonant material system into the cavity. Recently, normal mode splitting of semiconductor quantum dots in a photonic microcavity has been observed experimentally [2] by measuring the emission spectrum after non-resonant excitation into the continuum of wetting-layer states. In this context, an interesting question arises: Can one can see these coupling effects under resonant excitation conditions by measuring the reflected and/or transmitted signal?

In order to answer this question, we not only have to compute the electromagnetic field in and around the photonic crystal structure, but also model its excitation by a classical light source in the far field. The light-matter interaction inside the microcavity has to be computed self-consistently and the far field components of the transmitted and/or reflected fields as well as the corresponding spectra have to be evaluated. Specifically, we investigate a microcavity structure with a single defect into which we place a two-level atom being in resonance with the predominant cavity mode. This model is able to represent various physical implementations of two-level systems embedded in a photonic crystal at least to first order, hence the results are applicable to different experimental situations (nanocrystals, atoms, molecules).

2. The structure

The structure in our simulations is very similar to the one reported in Ref. [3]. It consists of a thin (thickness, $h = 0.348\mu m$) photonic crystal slab of semiconductor material, index $n = 3.4$, patterned with a triangular lattice (lattice constant $a = 0.464\mu m$) of air columns of radius $r = 0.275a$. Light is confined in the vertical (z) direction by total internal reflection at the interface between the slab and the air clad and in the in-plane direction by the photonic-bandgap effect. The slab is thin, less than the light wavelength, which ensures TE (dominant E_x, E_y, H_z components) single mode confinement in the vertical direction. The structure does not support a bandgap for TM modes.

A defect is introduced in the photonic crystal by reducing the radius of a single air column from $r = 0.275a$ to $r = 0.2a$ at the center of the lattice. This defect forms a nanocavity centered at the defect and is surrounded by six layers of air columns arranged in a hexagonal pattern, see, e.g., Fig. 4. The nanocavity supports a doubly-degenerate pair of donor defect eigenstates that can be separated into X and Y-dipole modes according to the orientation of the dominant electric field component at the center of the defect [3]. To increase the total Q of the cavity to ≈ 1500 an additional *fractional edge dislocation* defect of size $46.5nm$ is introduced through the central defect air column along the x-direction of the photon crystal lattice [4].

We place a two-level atom into the photonic crystal defect to study strong light-matter coupling. The optical response is modeled within the density matrix framework [5]. Assuming that only bound states ϕ_i are excited, the system can be described by the Hamiltonian:

$$H = \sum_i E_i a_i^+ a_i - \sum_{i,i'} \hbar\Omega_{i,i'}(t) a_i^+ a_{i'}.$$

where the electron creation and annihilation operators a_i^+ and $a_{i'}$, the level energies E_i and the Rabi frequency $\Omega_{i,i'}(t) = \vec{\mu}_{i,i'} \cdot \vec{E}(t)/\hbar$ with the optical dipole moment $\mu_{i,i'}$ have been introduced. Assuming that the extension of the atom is negligible compared to the wavelength of the electromagnetic field, the macroscopic polarization which enters the Maxwell equations can be written as:

$$\vec{P}_m(t,\vec{r}) = \delta(\vec{r} - \vec{r}_{atom}) \sum_{i,i'} \vec{\mu}_{i,i'} \langle a_i^+ a_{i'} \rangle.$$

In our numerical calculations, the δ-function is represented by a Gaussian distribution extending over several spatial grid cells. The equation of motion for the microscopic coherences

$\langle a_i^+ a_{i'} \rangle$ can be derived using the Heisenberg equation. Considering only linear excitation of the lowest transition (between levels 1 and 2) the dynamics of the relevant microscopic polarization $p = \langle a_1^+ a_2 \rangle$ is determined by [6]:

$$i\hbar \dot{p} = (E_2 - E_1)p + \Omega_{1,2}(t)$$

3. The simulation

We use a fourth order Runge-Kutta solver to numerically integrate the differential equation for the microscopic polarization. Since we want to have near resonant conditions, we choose the energy difference between the two optically coupled levels to be $(E_2 - E_1)/h = 190 THz$ in agreement with the dominant cavity mode frequency. In order to have strong light-matter coupling effects and to reduce the computational effort, we assume the relatively large dipole moment of $\mu_{12} = 12.5 enm$, however from scaling considerations we expect the results presented here to be transferable to similar systems in the strong coupling regime. The atomic dipole moment vector is chosen in the plane of the photonic crystal, parallel to the x-direction.
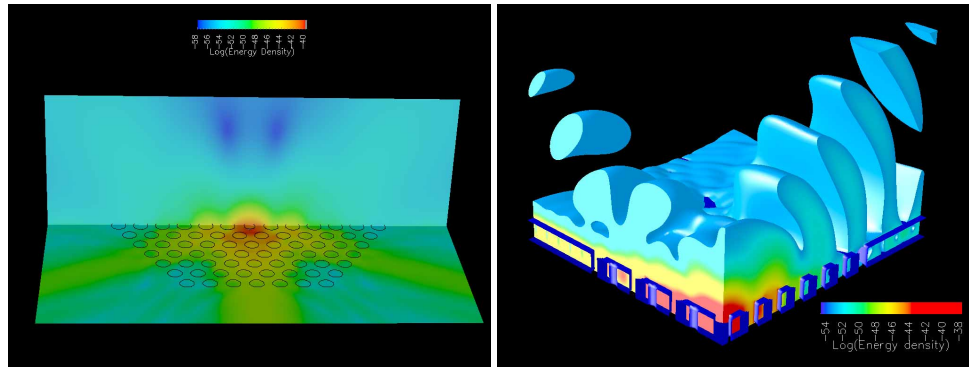

Fig. 1. Averaged (left) and time instantaneous (right) energy density W_0 of the electromagnetic field (1ps after excitation). Note the hexagonal symmetry of the evanescent field extending around the cavity and the radiation pattern above the structure. See also animation[11]. (mpeg, 1.2mb)

The electromagnetic field dynamics in the photonic crystal structure is simulated using a three dimensional FDTD (finite difference time domain) method where the computational grid is terminated with UPML (uniaxially perfectly matched layer) absorbing boundary conditions in all spatial directions [7]. A grid resolution of $\Delta = 23.25 nm$ is used which translates to 20 points per wavelength in the semiconductor slab. To improve simulation accuracy and offset errors due to the staircasing approximation of the air holes, which possess stronger curvature relative to the wavelength, an effective dielectric constant is computed for each cell on the air-semiconductor boundaries using a volume average of the dielectric constants at a resolution of $\Delta x/10$ [8]. However, the discretized representation should only be considered as an approximation to the geometrically defined structure.

4. Results

To analyze the optical properties of the 'empty' microcavity without an atom we artificially excite the structure using a transparent point dipole source located in the cavity region. To preferentially excite the X-dipole mode, the point polarization source is driven by a spectrally narrow pulse centered at the mode frequency and x-polarized. In order to focus on the eigenmodes of the cavity, all measurements are performed after the driving source is turned off and
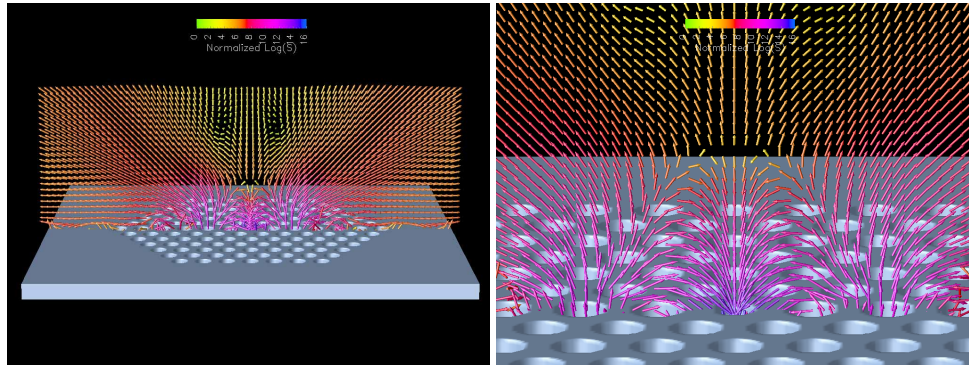
Fig. 2. Poynting vector in the x-z plane (1ps after excitation). Around the cavity a separatrix between near and far field can be seen. See also animation[11]. (mpeg, 2.4mb)

the rapidly decaying components have radiated away. In Fig. 1 we show a plot of the energy density of the electromagnetic field in the x-y and the x-z plane averaged over one period (left) and instantenous with carrier oscillations (right). Within the slab a hexagonal radiation pattern with strongly localized outgoing beams can be seen. Around the cavity a region with predominantly evanescent field components is visible. The far field emissions above the structure do not follow the hexagonal scheme and are much weaker compared to the in-plane losses.

Figure 2 shows the log of the time averaged local Poynting vector. The vectors are normalized by setting the length of the smallest one to unity. In the figure, we notice the appearance of a relatively well defined separatrix dividing the near field and propagating components. The electromagnetic flux is dynamically circulating between the inside of the photonic crystal structure and the near field region, whereas beyond the separatrix the fields are propagating away into the far field.
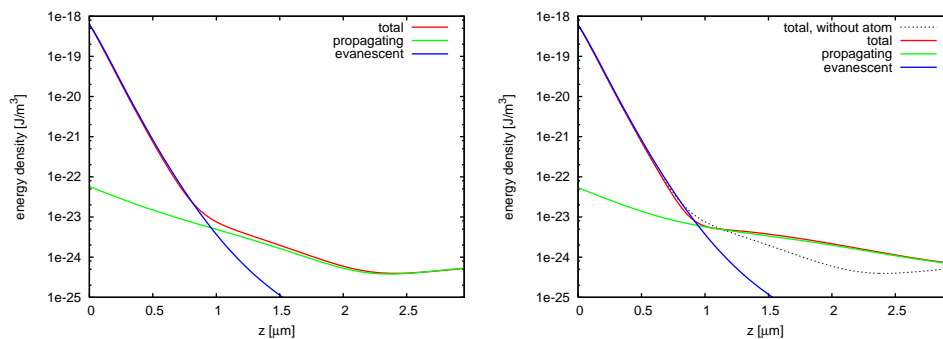

Fig. 3. Energy density of the propagating, evanescent and total parts of the electromagnetic field (1ps after excitation) in the z-direction above the photonic crystal structure with an empty cavity (left) and with atom (right). Around $1\mu m$ above the structure the propagating part (dominating the far-field) equals the evanescent part (dominating the near-field). Differences introduced due to the atom are most pronounced in the far-field (about $2\mu m$ above the structure).

For the air-filled half space above (or below) the structure a separation of the electromagnetic field into upward propagating and evanescent (localized) parts can be obtained by two-dimensional spatial Fourier transforms. Only the Fourier components lying within the light

cone ($|k_x|^2 + |k_y|^2 \le \omega_0/c$) can propagate into the upper far field, the remaining components only contribute to the near field and form the evanescent (inhomogeneous) field [9]. Figure 3 shows the energy density of the propagating, evanescent and total field along the vertical direction (z) above the center of the structure. Near the structure the evanescent part energetically dominates. However, since it falls of exponentially (note the logarithmic scale) the initially weaker but slower decaying propagating component is already of the same magnitude at a distance of about $1\mu m \approx 2/3\lambda$ above the structure and clearly dominates the far field.
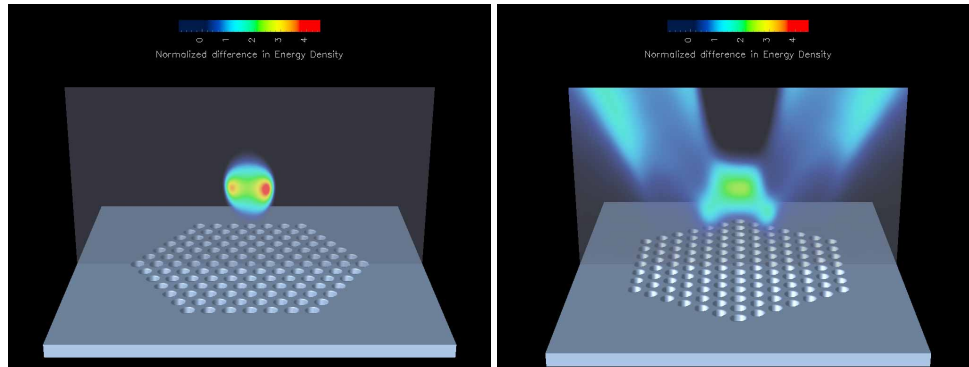

Fig. 4. Normalized difference $(W_{atom} - W_0)/W_0$ of the energy densities for simulations with (W_{qd}) and without (W_0) an atom in the defect in the x-z plane (left) and the y-z plane (right). The largest normalized differences occur about $2\mu m$ above the structure. See also animation[11]. (mpeg, 1.6mb)

Placing the atom into the cavity, i.e. into the defect of the structure, introduces a significant perturbation, particularly of the propagating field component. To visualize this effect, we show in Fig. 4 the normalized difference, i.e. one minus the energy density with atom divided by the energy density without atom. We notice a well defined region, approx $2\mu m$ above the plane of the photonic crystal, where the presence of the atom increases the energy density up to a factor of five.

To see the influence of the atom in a more quantitative way, we again separate the field into propagating and evanescent parts, see Fig. 3. Similar to the structure without the atom, the near-field is dominated by the evanescent part and the far-field consists mainly of propagating waves. While the overall signatures are very similar, there are considerable differences introduced by the atom. As can be seen in Fig. 3, these differences mainly occur in the propagating part of the electric field, which is to some part counter-intuitive as one would expect the influence to be stronger in the near-field region of the atom. These results reflect the cavity mode's property of having a finite lifetime (and hence Q). This lossiness requires the mode profile to have not only near field but also far field components, in which the signatures of the atom can be observed.

It is well known that a two level system coupled to a cavity mode can exhibit normal mode splitting, also known as vacuum Rabi splitting [10]. This splitting can be observed in the spectral response of the system if it is energetically larger than the typical linewidths of the two-level system and the cavity mode (non-perturbative coupling regime). For the considered system, Fig. 5 shows the intensity spectrum of the reemitted light (3ps after the incident pulse has left the system) as detected $3\mu m$ below the structure (transmission direction) for excitation with a plane wave pulse. The spectrum shows, that in comparison to the single mode for the empty cavity, the coupled system exhibits two modes with are spectrally separated by 873 GHz. As expected, the new linewidth is the average of the original cavity mode and atom linewidths.

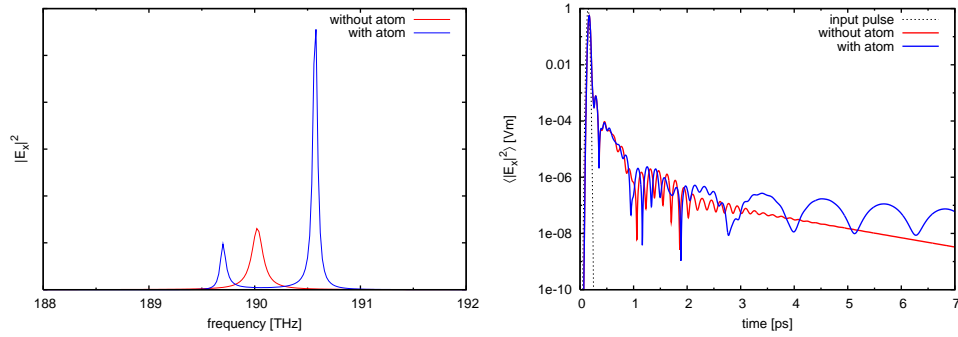The corresponding temporal dynamics of the system is shown in Fig. 5. In addition to the

Fig. 5. Left: Spectrum of the structure's emission with and without atom. A normal mode splitting of 873GHz can be observed. Right: Temporal intensity envelope with and without atom normalized to input pulse maximum. With the atom a beating which corresponds to the normal mode splitting occurs.

directly transmitted part of the pulse, the displayed time averaged intensity shows several oscillations originating from radiation of short lived modes of the photonic crystal during the first few picoseconds. Subsequently, the system without atom settles into a single slowly decaying mode. With the atom a temporal beating of the two cavity polariton modes evolves with an even slower decay rate.

We would like to note that calculations for the experimental configuration of Ref. [2] have also been conducted showing quantitative agreement with the reported splitting. However, the available data only allowed a multiexponential analysis instead of a full Fourier transformation and it was not feasible to calculate the extended field patterns which constitute the focus of the present paper.

5.   Conclusions

In this paper we present extended numerical simulations of the electromagnetic field properties of a photonic crystal nanocavity with and without a resonant atom. Even though the high Q cavity modes are strongly localized around the photonic crystal structure, each mode has a well defined component that travels into the far field. Hence, the cavity mode can be analyzed using a plane wave source and measuring the transmitted and/or reflected field. From the Fourier transform of a transmitted short pulse, we obtain the normal mode splitting introduced by the non-perturbative coupling between the atom and the cavity mode.